Clean Technol., Vol. 24, No. 3, September 2018, pp. 206-211

청정환경기술

Photocatalytic Decomposition of Rhodamine B on $PbMoO_4$ Using a Surfactant-assisted Hydrothermal Method

Seong-Soo Hong*

Department of Chemical Engineering, Pukyong National University
45 Yongso-ro, Nam-gu, Busan, 48513 Korea

(Received for review May 1, 2018; Revision received June 5, 2018)

Abstract

Lead molybdate ($PbMoO_4$) were successfully synthesized using a facile surfactant-assisted hydrothermal process and characterized by XRD, Raman, PL, BET and DRS. We also investigated the photocatalytic activity of these materials for the decomposition of Rhodamine B under UV-light irradiation. From XRD and Raman results, well-crystallized $PbMoO_4$ crystals have been successfully synthesized with a facile surfactant-assisted hydrothermal process and had 52-69 nm particle size. The $PbMoO_4$ catalysts prepared at 160 ℃ showed the highest photocatalytic activity. The PL peak was appeared at about 540 nm at all catalysts and it was also shown that the excitonic PL signal was proportional to the photocatalytic activity for the decomposition of Rhodamine B.

Keywords : Lead molybdate ($PbMoO_4$), Surfactant-assisted hydrothermal process, Photocatalytic decomposition of Rhodamine B

1. Introduction

Semiconductor photocatalysts on a nanometer-scale have become more and more attractive because of their different physical and chemical properties from bulk materials [1,2]. The surface structure of photocatalysts play an important role to their photocatalytic activities because the photocatalytic reaction or photoelectron conversion takes place only when photoinduced electrons and holes are available on the surface [3]. For example, both theoretical and experimental studies have demonstrated that the {001} facets of anatase TiO_2 are much more reactive than the thermodynamically more stable {101} facets [4]. Therefore, the surface controlled fabrication of nanocrystals is not only a rational route to study the relations between the surface structures and the photocatalytic properties but also a feasible approach for developing highly active photocatalysts.

Metal molybdate and metal tungstate materials as a scheelite structure have wide potential and practical applications in many fields, e.g. photoluminescence (PL), solid-state optical maser, optical fibers, scintillator materials, humidity sensor, magnetic materials and catalysts [5,6]. $PbMoO_4$ and $SrMoO_4$ crystallize in this so-called scheelite structure, which belong to the tetragonal space group $I4_1/a$ [5]. They have been reported due to the above mentioned applications. $PbMoO_4$ has also been reported as a photocatalyst for the splitting of water [7]. Unfortunately, almost all of the $PbMoO_4$ crystals synthesized by traditional solid state reactions and solution phase methods are dominated by irregular shape and large crystal size due to its rapid crystal growth feature [8]. Recently, Zheng and co-workers have reported γ-Bi_2MoO_6 sheets with preferentially exposed (010) crystal facets exhibiting greatly enhanced photoactivity in comparison with γ-Bi_2MoO_6 nanoparticles and sheets with preferentially exposed (131) crystal facets, and found that the exposed (010) faces containing much more oxygen defects are beneficial for suppressing the photogenerated carriers recombination and promoting the generation of OH radical [9]. The above investigations remind us that the photocatalytic activity of photocatalysts can be tailored by controlling their exposed crystal facet and morphology. Therefore, the controllable preparation of photocatalysts with different morphologies and exposed crystal facets is still very important and challenging. Shen and co-workers have reported that the surfactant on the preparation of $PbMoO_4$ played an important role in the formation of preferentially exposed crystal facets to enhance the photocatalytic activity [10]. Therefore, the preparation of uniform, high-purity $PbMoO_4$ nanocrystals with

* To whom correspondence should be addressed.
E-mail: sshong@pknu.ac.kr; Tel: +82-51-629-6433; Fax: +82-51-629-6429

doi: 10.7464/ksct.2018.24.3.206 pISSN 1598-9712 eISSN 2288-0690

controllable crystallographic facets can be obtained using a facile surfactant-assisted hydrothermal process.

In this paper, we prepared nanosized $PbMoO_4$ particles using a facile surfactant-assisted hydrothermal process. The synthesized materials were characterized using XRD, DRS, PL, BET and Raman. Their activity as photocatalysts for the decomposition of Rhodamine B was investigated. In addition, the optimal experiment conditions for the preparation were investigated to get the high photocatalytic activity.

2. Experimental

In a facile surfactant-assisted hydrothermal process, $(NH_4)_6Mo_7O_{24}\cdot 4H_2O$ (5.3 g), $Pb(NO_3)_2\cdot 4H_2O$ (9.94 g) and cetyltrimethyl ammonium bromide (CTAB) were used as the starting materials without further purification. The appropriate amounts of starting materials were dissolved in distilled water (120 mL) and added into a Teflon-lined steel autoclave of 150 mL. Then 24 g of ethylene glycol was added. Under stirring, 4 mol L^{-1} of NaOH solution was used to adjust that the pH value is 9, and the autoclave was heated under autogenous pressure at from 100 to 180 ℃ for 12 h. The resulting solid powders were collected, and washed with deionized water and ethanol, and then they were dried at the 120 ℃ for 12 h. In order to investigate the effect of calcination temperature on the morphology and the crystal facets of $PbMoO_4$, the temperature was changed from 200 to 500 ℃.

The crystal structures of the prepared $PbMoO_4$ materials were examined by powder X-ray diffraction (XRD) with Cu-Kα radiation (Rigaku Co. Model DMax). The BET surface area of the prepared particles was determined by nitrogen physisorption data at 77 K using a Quantachrome NOVA 1000. UV-vis diffuse reflectance spectroscopy (DRS) was performed on a Varian Cary 100 using PTFE (polytetrafluoroethylene) as a standard. The micro-Raman (MR) spectra of the products were obtained with a Raman spectrometer (Dimension-pl-Raman, USA) with a radiation of 532 nm from an argon ion laser. Photoluminescence (PL) spectra were examined using a fluorescence spectrophotometer (KIMMON KOHA, Japan) with Xe lamp (power: 350 W) as the light source at room temperature.

The photocatalytic reactions were performed with a 300 W Xe-arc lamp (Oriel). Light was passed through a 10 cm IR water filter and then focused onto a 100 mL pyrex with a quartz window. The reactor was filled with 100 mL of an aqueous dispersion in which the concentrations of the photocatalyst and Rhodamine B were 1 g L^{-1} and 10 mg L^{-1}, respectively. This solution was magnetically stirred that the concentration and temperature remained uniform. The samples were immediately centrifuged and the quantitative determination of Rhodamine B was performed using a UV-vis spectrophotometer (Mecasys Optizen Pop).

3. Results and discussion

Figure 1 shows the XRD patterns of $PbMoO_4$ catalysts prepared using hydrothermal process at different preparation temperature. The temperature was changed from 100 to 180 ℃. Their XRD patterns revealed that the products can be indexed as the tetragonal structure with space group $I4_1/a$ regardless of the preparation temperature, in agreement with the respective JCPDS No. 08-0475 for $PbMoO_4$.

The experimental lattice parameters were calculated using the equation of plane spacing for the tetragonal structure and Bragg's law for diffraction [11]. They are a = 5.4070 Å and c = 12.0388 Å for $PbMoO_4$. The approximate crystallite sizes of $PbMO_4$ were calculated from (112) peak of XRD patterns with Scherrer's equation [11].

$$D = 0.9\lambda / \beta\cos\theta$$

where D is the crystallite size in nm, λ is the radiation wavelength (0.15405 nm for CuK_α), β is corrected half-width, and

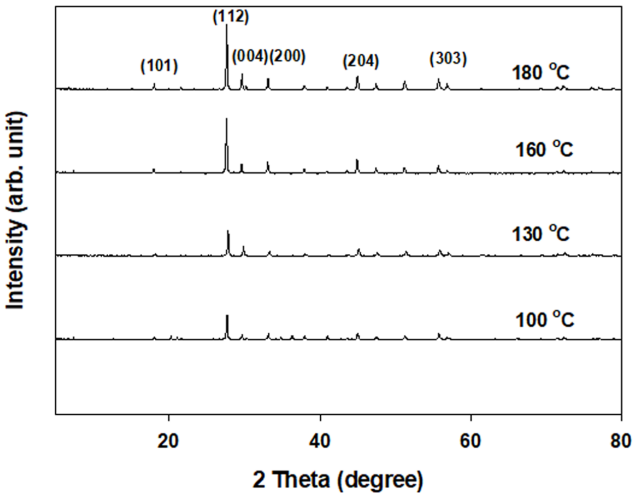

Figure 1. X-ray diffraction patterns of $PbMoO_4$ catalysts prepared using hydrothermal process at different preparation temperature.

Table 1. The physical properties and photocatalytic activity of $PbMoO_4$ catalysts prepared at different preparation temperature

Preparation temperature (℃)	Particle size (nm)	Surface area ($m^2\ g^{-1}$)	k [a] ($\times 10^{-3}\ min^{-1}$)
100	52	3.0	50.3
130	56	2.8	67.1
160	59	2.6	121.8
180	59	2.6	71.4

[a] apparent first-order constant (k_{app}) of photocatalytic degradation of Rhodamine B

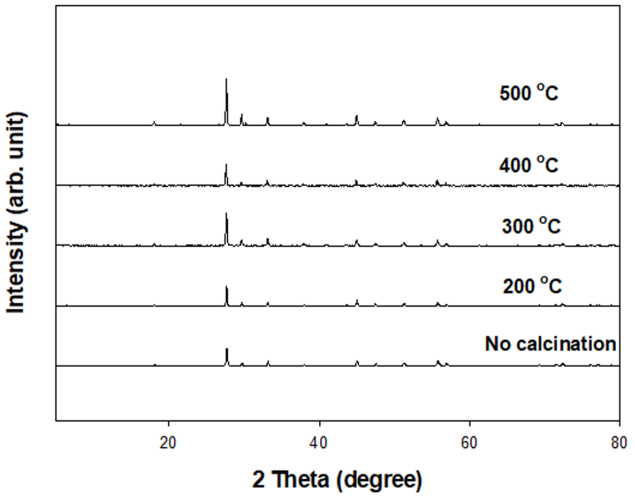

Figure 2. X-ray diffraction patterns of $PbMoO_4$ catalysts prepared using hydrothermal process at different calcination temperature.

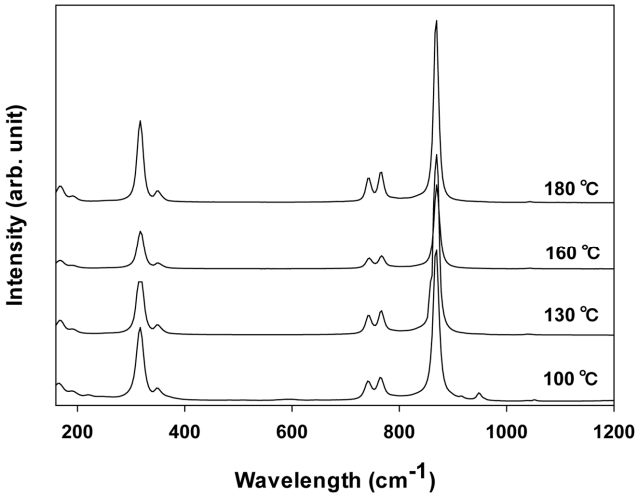

Figure 3. Raman spectra of $PbMoO_4$ catalysts prepared using hydrothermal process at different preparation temperature.

Table 2. The physical properties and photocatalytic activity of $PbMoO_4$ catalysts calcined at different temperature

Calcination temperature (℃)	Particle size (nm)	Surface area ($m^2\ g^{-1}$)	k [a] ($\times 10^{-3}\ min^{-1}$)
No calcination	52	2.6	121.8
200	56	2.5	90.3
300	59	2.4	19.4
400	63	2.4	10.1
500	69	2.2	5.2

[a] apparent first-order constant (k_{app}) of photocatalytic degradation of Rhodamine B

θ is the diffraction peak angle. The average crystallite sizes of all samples are calculated by Scherrer's equation as shown in Table 1. The crystallite size increased from 52 to 59 nm with an increase of preparation temperature.

Figure 2 shows the XRD patterns of $PbMoO_4$ catalysts prepared using hydrothermal process at different calcination temperature. Their XRD patterns also revealed that the products can be indexed as the tetragonal structure with space group $I4_1/a$ regardless of the calcination temperature. As shown in Table 2, the crystallite size increased from 52 to 69 nm with an increase of calcination temperature.

Figure 3 shows the Raman spectra in the range from 150 to 1000 cm^{-1} of $PbMoO_4$ catalysts prepared using hydrothermal process at different preparation temperature. The Raman peak at 869.5 cm^{-1} was assigned to the symmetric stretching vibration mode ν_1 (A_g) of the $[MoO_4]$ clusters in the $PbMoO_4$ crystal [12]. The peaks at 767.0 and 741.2 cm^{-1} corresponded to the anti-symmetric stretching ν_3 (B_g) and ν_3 (E_g) vibration modes, respectively. Two modes at 347.6 and 317.2 cm^{-1} were interpreted as the weaker ν_4 (B_g) and stronger ν_2 (A_g) of the regular $[MoO_4]^{2-}$ tetrahedrons. The A_g mode at 166.5 cm^{-1} for $PbMoO_4$ is much weaker than other modes. These results were consistent with other reports about $PbMoO_4$ [6,12]. No peaks in the XRD or Raman spectra from other impurities were detected. Therefore, it is reasonable to conclude that well-crystallized $PbMoO_4$ crystals have been successfully synthesized with the hydrothermal method regardless of the preparation temperature.

The light absorption properties of the photocatalysts were examined by diffuse reflectance UV–Vis spectroscopy. Figure 4 shows the UV–Vis diffuse reflectance spectra of $PbMoO_4$ catalysts prepared using hydrothermal process at different preparation temperature. As shown in Figure 4, all the catalysts displayed similar absorption spectrum in the UV light region re-

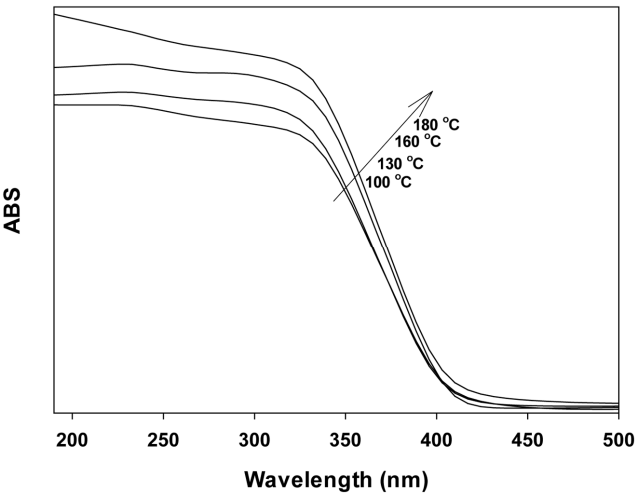

Figure 4. UV-Vis diffuse reflectance spectra of $PbMoO_4$ catalysts prepared using hydrothermal process at different preparation temperature.

gardless of the preparation temperature. However, the absorption edge of the sample moved slightly to higher wavelength with an increase of preparation temperature, which can be ascribed to the increase of grain size. From the onset of the absorption edge in Figure 4, the band gap is estimated at about 3.20 eV, which can be ascribed to the characteristic absorption of $PbMoO_4$ [13]. The band structure of $PbMoO_4$ was suggested to be composed of Mo_{4d} (conduction band, CB) and hybridization of O_{2p} and Pb_{6s} (valence band, VB) according to other research [13,14].

It is well known that photocatalytic oxidation of organic pollutants follows Langmuir-Hinshelwood kinetics [15], where the rate is proportional to the coverage θ:

$$r = -\frac{dc}{dt} = k\theta = k\frac{KC}{1 + KC} \quad (1)$$

where k is the true rate constant which is dependent upon various parameters such as mass of the catalyst, the flux efficiency, oxygen coverage, etc., K is the adsorption coefficient of the reactant, and C is the reactant concentration. When C is very small, the product KC is negligible with respect to unity and under these conditions Equation (1) describes a first-order kinetic reaction. Setting the parameters in Equation (1) to the initial conditions of the photocatalytic procedure, $t=0$, the concentration can be given as $C=C_0$, which results in Equation (2).

$$-ln\left(\frac{C}{Co}\right) = k_{app}t \quad (2)$$

where k_{app} is the apparent first-order reaction constant.

The photocatalytic activity for the decomposition of Rhodamine B over $PbMoO_4$ catalysts prepared using hydrothermal process at different preparation temperature is shown in Figure 5 and Table 1. When a blank test was carried out in the absence of the photocatalyst, about 2% of the Rhodamine B was decomposed after 2 h by the photolysis reaction. As shown in Figure 5, the photocatalytic activity increased with increasing preparation temperature and Rhodamin B was completely decomposed within 30 min on the $PbMoO_4$ catalysts prepared at 160 ℃. However, the activity of $PbMoO_4$ catalyst prepared at 180 ℃ was decreased.

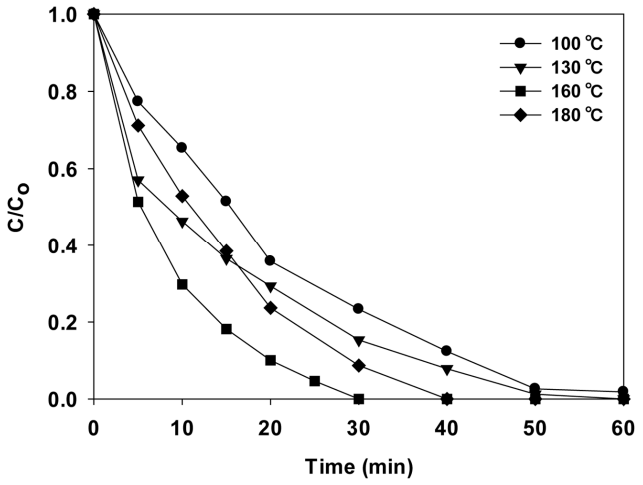

Figure 5. Photocatalytic decomposition of Rhodamine B over $PbMoO_4$ catalysts prepared using hydrothermal method at different preparation temperature.

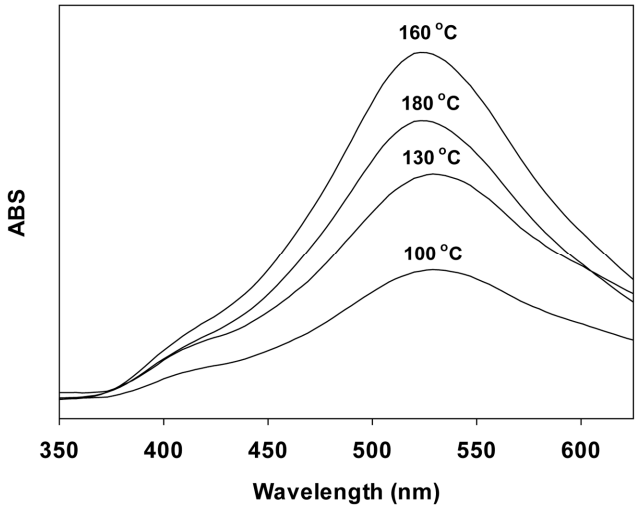

Figure 6. PL spectra of $PbMoO_4$ catalysts prepared using hydrothermal method at different preparation temperature.

Figure 6 shows the PL spectra of $PbMoO_4$ catalysts prepared using hydrothermal process at different preparation temperature. It is shown that the $PbMoO_4$ samples can obvious excitonic PL signals with similar shape regardless of preparation temperature. In addition, the excitonic PL signal shows the highest intensity in the case of $PbMoO_4$ catalyst prepared at 160 ℃. It is well known that $PbMoO_4$ materials exhibit the strong and wide PL signals at the range from 500 to 600 nm with the excited wavelength of 300 nm. For the $PbMoO_4$ catalysts, one obvious PL peak is appeared at about 540 nm. It is known that the emission spectrum of the metal molybdates might be ascribed to the charge-transfer transitions within the $[MoO_4]$ clusters [16]. The stronger the excitonic PL signal, the higher the content of surface oxygen vacancy and defect. In addition, during the process of the photocatalytic reaction, oxygen vacancy and defect can become the centers to capture photo-induced electrons so that the recombination of photo-induced electrons and holes can be inhibited. Moreover, oxygen vacancies can promote the adsorption of oxygen and then the strong interaction between the photo-induced electrons bound by oxygen vacancies and adsorbed oxygen can be formed. This result indicates that the binding for the photo-induced electrons of oxygen vacancies can make the capture for photo-induced electrons of adsorbed oxygen and oxygen radical group was produced at the same time. Therefore, oxygen

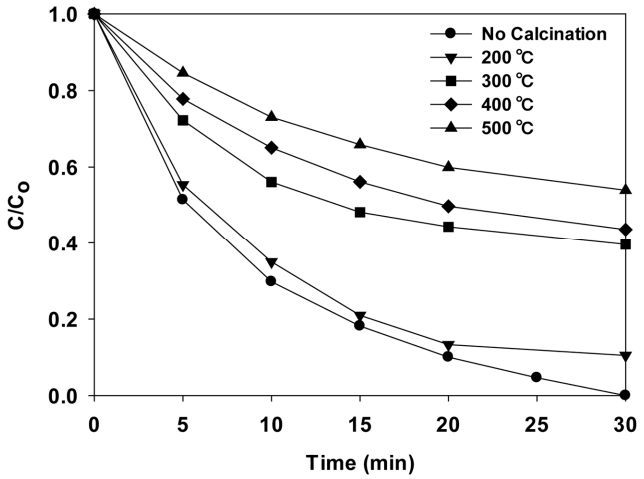

Figure 7. Photocatalytic decomposition of Rhodamine B over $PbMoO_4$ catalysts prepared using hydrothermal method at different calcination temperature.

vacancy and defect are in favor of photocatalytic reactions in that oxygen is active to promote the oxidation of organic substances. This suggests that the stronger the PL intensity, the larger the amount of oxygen vacancy and defect, the higher the photocatalytic activity. As shown in Figure 6, the photocatalytic activity on the decomposition of Rhodamine B shows the same order with the intensity of PL peaks of $PbMoO_4$ catalysts.

Figure 7 shows the photocatalytic activity for the decomposition of Rhodamine B over $PbMoO_4$ catalysts prepared by different calcination temperature. As shown in Figure 7 and Table 2, the photocatalytic activity was decreased with an increase of calcination temperature and the $PbMoO_4$ catalyst prepared without a calcination process showed the highest activity.

Figure 8 shows the PL spectra of $PbMoO_4$ catalysts prepared using different calcination temperatures. $PbMoO_4$ samples showed one obvious excitonic PL signals at 540 nm regardless of the calcination temperature. The excitonic PL signal increased with decreasing calcination temperature. Furthermore, the photocatalytic activity for the decomposition of Rhodamin B also showed the same order with the intensity of PL peaks of $PbMoO_4$ catalysts prepared at different calcination temperatures. As afore-mentioned, this result also verified that the stronger the PL intensity, the higher the photocatalytic activity.

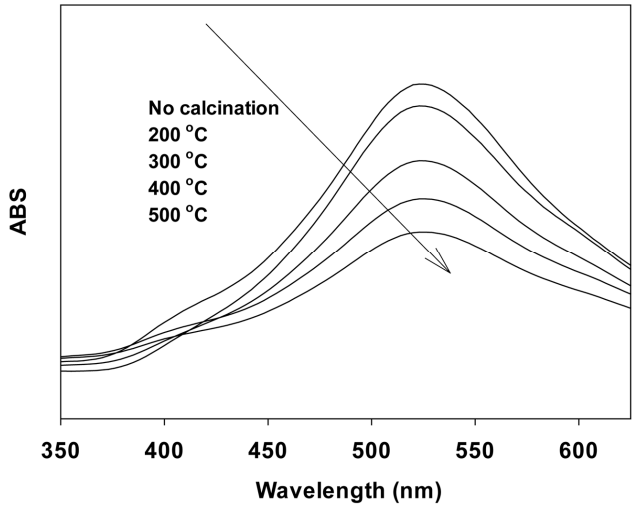

Figure 8. PL spectra of $PbMoO_4$ catalysts prepared using hydrothermal method at different calcination temperature.

4. Conclusions

In this study, we have investigated the photocatalytic activity of lead molybdate ($PbMoO_4$) scheelite-type oxides prepared using a facile surfactant-assisted hydrothermal process on the decomposition of Rhodamine B. From the XRD and Raman results, the formation of the well-crystallized $PbMoO_4$ phase was confirmed for all catalysts regardless of preparation temperature. The photocatalytic activity increased with increasing preparation temperature and Rhodamine B was completely decomposed within 30 min on the $PbMoO_4$ catalysts prepared at 160 ℃. In addition, the photocatalytic activity was decreased with an increase of calcination temperature and the $PbMoO_4$ catalyst prepared without a calcination process showed the highest activity. The PL peak was appeared at about 540 nm at all catalysts and it was also shown that the excitonic PL signal was proportional to the photocatalytic activity for the decomposition of Rhodamine B.

References

1. Wang, Z. C., Medforth, C. J., and Shelnutt, J. A., "Self-metallization of Photocatalytic Porphyrin Nanotubes," *J. Am. Chem. Soc.*, **126**, 16720-16721 (2004).
2. Li, H. X., Bian, Z., Zhu, J., Huo, Y., Li, H., and Lu, Y., "Mesoporous Au/TiO_2 Nanocomposites with Enhanced Photocatalytic Activity," *J. Am. Chem. Soc.*, **129**, 4538-4539 (2007).
3. Hameed, A., Montini, T., Gombac, V., and Fornasiero, P., "Surface Phases and Photocatalytic Activity Correlation of Bi_2O_3/Bi_2O_{4-x} Nanocomposite," *J. Am. Chem. Soc.*, **130**, 9658-9659 (2008).
4. Han, X. Q., Kuang, Q., Jin, M. S., Xie, Z. X., and Zheng, L. X., "Synthesis of Titania Nanosheets with a High Percentage of Exposed (001) Facets and Related Photocatalytic Properties," *J. Am. Chem. Soc.*, **131**, 3152-3152 (2009).
5. Mao, C. J., Geng, J., Wu, X. C., and Zhu, J. J., "Selective Synthesis and Luminescence Properties of Self-Assembled $SrMoO_4$ Superstructures via a Facile Sonochemical Route," *J. Phys. Chem. C*, **114**, 1982-1988 (2010).
6. Phuruangrat, A. Thongtemb, T., and Thongtem, S., "Synthesis of Lead Molybdate and Lead Tungstate via Microwave Irra-

diation Method," *J. Cryst. Growth*, **311**, 4076-4081 (2009).
7. Kudo, A., Steinberg, M., Bard, A. J., Campion, A., Fox, M. A., Mallouk, E., Webber, S. E., and White, J. M., 'Photoactivity of Ternary Lead-group IVb Oxides for Hydrogen and Oxygen Evolution," *Catal. Lett.*, **5**, 61-66 (1990).
8. Sayama, K., Nomura, A., Zou, Z. G., Abe, R., Abe, Y., and Arakawa, H., "Photoelectrochemical Decomposition of Water on Nanocrystalline $BiVO_4$ Film Electrodes under Visible Light," *Chem. Commun*., **99**, 2908-2909 (2003).
9. Zheng, Y., Duan, F., Wan, J., Liu, L., Chen, M. Q., and Xie, Y., "Enhanced Photocatalytic Activity of Bismuth Mlybdates with the Preferentially Exposed {010} Surface under Visible Light Irradiation," *J. Mol. Catal. A: Chem.*, **303**, 9-14 (2009).
10. Shen. M., Zhang, Q., Chen, H., and Peng, T., 'Hydrothermal Fabrication of $PbMoO_4$ Microcrystals with Exposed (001) Facets and Its Enhanced Photocatalytic Properties," *Crust. Eng. Comm*, **13**, 2785-2791 (2011).
11. Cullity, B. D., Elements of X-Ray Diffraction, Adison-Wesley, Reading, MA, 213 (1978).
12 Sczancoski, J. C., Bomio, M. D. R., Cavalcante, L. S., Joya, M. R., Pizani, P. S., Varela, J. A., Longo, E., Li, M. S., and Andre's, A., "Morphology and Blue Photoluminescence Emission of $PbMoO_4$ Processed in Conventional Hydrothermal," *J. Phys. Chem. C*, **113**, 5812-5822 (2009).
13. Shimodaira, Y., Kato, H., Kobayashi, H., and Kudo, A., "Investigations of Electronic Structures and Photocatalytic Activities under Visible Light Irradiation of Lead Molybdate Replaced with Chromium (VI)," *Bull. Chem. Soc. Jpn.*, **80**, 885-893 (2007).
14. Bi, J. H., Wu, L., Zhang, Y. F., Li, Zh. H., Li, J. Q., and Fu, X., "Solvothermal Preparation, Electronic Structure and Photocatalytic Properties of $PbMoO_4$ and $SrMoO_4$," *Appl. Catal. B*, **91**, 135-143 (2009).
15. Jung, W. Y., and Hong, S. S., "Synthesis of $LaCoO_3$ Nanoparticles by Microwave Process and Their Photocatalytic Activity under Visible Light Irradiation," *J. Ind. &Eng. Chem*., **19**, 157-160 (2013).
16. Sczancoski, J. C., Cavalcante, L. S., Marana, N. L., daSilva, R. O., Tranquilin, R. L., Joya, M. R., Pizani, P. S., Varela, J. A., Sambrano, J. R., Li, M. S., Longo, E., and Andre's, J., "Electronic Structure and Optical Properties of $baMoO_4$ Powders," *Curr. Appl. Phys.*, **10**, 614-624 (2010).